Am J Transl Res 2026;18(1):179-189
www.ajtr.org /ISSN:1943-8141/AJTR0165365

Original Article

Effects of Micro-Arc oxidation treatment on the osseointegration of microscrews in bone tissue

Yawen Dai[1*], Yufei Ren[2*], Wantian Xu[1#], Lin Liu[3#]

[1]Nanjing Stomatological Hospital, Affiliated Hospital of Medical School, Research Institute of Stomatology, Nanjing University, Nanjing, Jiangsu, China; [2]Department of Stomatology, Nanjing Integrated Traditional Chinese and Western Medicine Hospital, Nanjing, Jiangsu, China; [3]Department of Orthodontics, Dalian Stomatological Hospital, Graduate School of Dalian Medical University, Dalian, Liaoning, China. [*]Equal contributors and co-first authors. [#]Equal contributors.

Received April 15, 2025; Accepted December 7, 2025; Epub January 15, 2026; Published January 30, 2026

Abstract: Objective: This study aimed to examine the surface morphology and physical properties of micro-screws following micro-arc oxidation surface treatment, and to verify the findings using an animal experimental model. Methods: A comparative analysis was conducted between micro-arc oxidized micro-screws (Group B) and conventional micro-screws (Group A). Suitable animal subjects were selected in accordance with experimental criteria. All experimental measured data were subjected to statistical analysis. Results: 1) The threaded portion of micro-screws in Group B exhibited better wettability and roughness compared to those in Group A, along with good coating adhesion. 2) Both the new bone mass and bone combination rate for Group B micro-screws showed an upward trend. Conclusion: The study demonstrated that micro-arc oxidation treatment enhanced the surface wettability and roughness of the micro-screws and significantly increased bone formation, suggesting improved stability following treatment.

Keywords: Orthodontic microscrews, Micro-Arc oxidation, osseointegration, surface treatment, stability

Introduction

The design and control of orthodontic support are directly linked to treatment efficacy. Traditional orthodontic support often yields uncertain results. The introduction of various implant support systems has enhanced the design of traditional orthodontic support, broadened its, and marked a turning point for orthodontic concepts as well as clinical diagnosis and treatment. Due to their small size, flexibility in implantation, ease of operation, and minimal mucosal damage to patients, micro-screws are widely favored in orthodontic treatment [1].

However, micro-screw dislodgement remains a challenge for both doctors and patients. Studies have reported a success rate of only 74% for micro-implant microscrews [2], and their stability is influenced by multiple factors, such as material composition, shape, implantation site, loading time, patient's bone quality, and oral hygiene [3-5].

In recent years, researchers worldwide have explored various implant surface treatments to enhance the osseointegration and stability of the implant. These treatments include acid-etching, sandblasting, hydroxyapatite coating, micro-arc oxidation, and ultraviolet light functionalization [6-8]. Among these, micro-arc oxidation (MAO) technology has emerged as one of the most widely adopted implant surface modification techniques owing to its ease of operation, low cost, and the ability to precisely and effectively adjust the microstructure and elements of the prepared surface coatings. This process significantly improved the biocompatibility and osteoconductivity of pure titanium implants [9].

MAO, also referred to as plasma electrolytic oxidation (PEO) or anodic spark deposition (ASD), is an anodic oxidation process in which a high-voltage power supply generates instantaneous high temperatures and voltages on its anode surface. This leads to arc discharge in the electrolyte, inducing the formation of a bioactive

https://doi.org/10.62347/GUSX6216

TiO_2 coating on the anode surface [10, 11]. The newly formed TiO_2 layer is both porous and rough, enabling integration with the bone and firm adhesion to the substrate. This process enhances the biological properties of the implant and improves interfacial bonding between the bone tissue and Ti or its alloys. Recent studies have shown that MAO is highly effective in modifying Ti implants [12-14].

Materials and methods

Characterization of micro-implant microscrews after MAO surface treatment

Experimental materials

A total of 60 orthodontic micro-implant microscrews (Φ1.5 × 6.0 mm, thread length 6.0 mm, pitch 0.6 mm) were prepared, produced by Hangzhou Pute Medical Instrument Co. Group A (control group) consisted of 30, while Group B (experimental group) consisted of 30 microscrews subjected to MAO surface treatment.

Experimental steps

MAO surface treatment of micro-implant microscrews: The 30 micro-implant microscrews (Ti-6Al-4V) in Group B were ultrasonically cleaned in anhydrous ethanol for 5 min. Next, the threaded part of the micro-implant microscrews was subjected to MAO treatment using a WHD-20 micro-arc oxidation power supply with the micro-implant microscrew as the anode and the stainless steel electrolytic tank as the cathode. The treatment parameters were as follows: voltage 350 V, frequency 600 Hz, duty cycle 9%, and electrolyte temperature maintained below 50°C. The electrolyte consisted of an aqueous solution of 0.1 mol/L $Li_2B_4O_7$ and 0.05 mol/L NaF. The MAO treatment was applied for 10 seconds. Notably, 1/3rd of the tips of the microscrews were left untreated to preserve their strength and sharpness.

Detection of surface properties of micro-implant microscrews: A field emission scanning electron microscope (Supra 55, Germany) was used to analyze and compare the surface coating morphology of the threaded part of the microscrews in both groups. A field emission electron microprobe (JXA-8530F PLUS, Japan) was employed to determine the surface elemental composition. An X-ray diffractometer (Empyrean, The Netherlands) was used to measure the surface phase structure of the two groups of microscrews, while a contact angle meter (DSA100, Germany) was used to measure the contact angle of the microscrew surfaces. A laser confocal microscope (OLS4000, Japan) was employed to measure the three-dimensional features of the two microscrew surfaces and to compare the surface roughness. Finally, a cross-hatch adhesion tester was used to examine the adhesion between the coating and the substrate in Group B microscrews.

Animal experiments to determine the effect of MAO surface-treated micro-implant microscrews on bone tissue

Experimental procedure

Nine healthy male New Zealand white rabbits, aged 4 to 5 months and weighing (2.58±0.18) kg, were selected and randomly numbered 1 to 9. The rabbits were reared in individual cages under controlled conditions (temperature around 25°C and humidity 60% to 65%). All experimental animals underwent surgery after being adaptively raised for 1 weeks. The experimental rabbits, feed, housing, and surgical procedures were provided by the Laboratory Animal Center of Dalian Medical University. This study was reviewed and approved by the Ethics Committee of Dalian Medical University (Approval Number: AEE23100).

First, the rabbits were anesthetized by intramuscular injection of rabbit tachyzoin II. After preparing the skin, bilateral incisions were made in the mid-tibial region of the hind legs to separate the muscle layer and expose the bone surface. Two Group A microscrews were implanted into the bone surface of the left hind leg, and two Group B microscrews were implanted into the right hind leg using the non-assisted method, maintaining a spacing of 14.5 mm. Next, nickel-titanium tension springs were applied to exert a force of 200 g. Postoperatively, the rabbit was treated with a cephalosporin II and Cefazolin (0.25 g/d) injection for three consecutive days.

Three experimental rabbits were sacrificed at 4, 8, and 12 weeks after the operation using

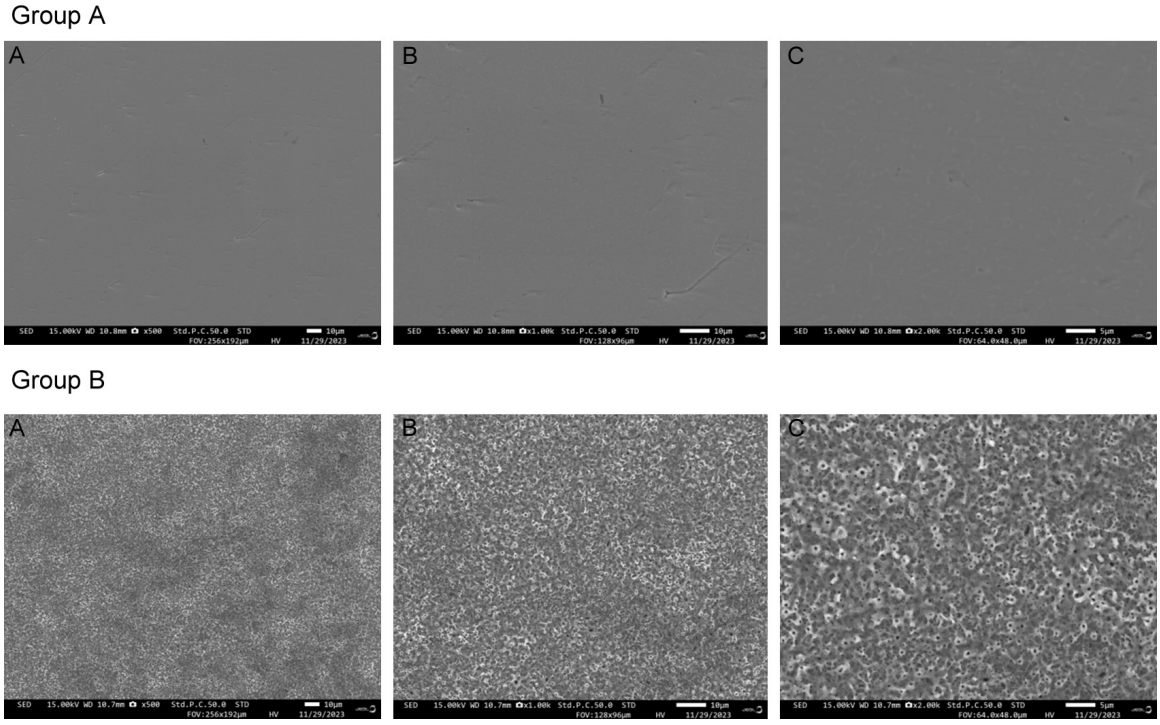

Figure 1. The upper three panels show the SEM characterization of group A microscrews (A) 500× (B) 1000× (C) 2000×. The lower three panels show the SEM characterization of group B microscrews (A) 500× (B) 1000× (C) 2000×.

the air embolism method. First, the rabbit was fixed in position and a vein on one side was exposed. A syringe was used to rapidly inject 30 mL of air into the vein, resulting in an air embolism in a pulmonary or coronary artery, ultimately causing circulatory obstruction, shock, and death. After hard tissue samples containing the microscrews were collected. None of the micro-implant microscrews were loosened or dislodged. All hard tissue samples were plastic-embedded and sectioned for analysis.

Specimen processing

The hard tissue specimens were fixed in 10% neutral formalin, dehydrated and transparent, and then polymerized for embedding. Next, the embedded tissue blocks were sectioned into 200-μm-thick thin slices with a hard tissue slicer (EXAKT 300CP, Germany). The slices were then polished with an EXAKT 400CS slicer (Germany) using abrasive paper of various mesh sizes (such as K320, K800, K1200, K4000) and finally ground into 20-μm-thick slices.

Setting parameters for morphometric analysis of new bone

The parameters for the morphological analysis of new bone were set using the Osteo-Measure analysis software, including B. ARr (new bone area), B. PAM (new bone circumference), BV/TV (volume ratio), Tb.Th (trabecular thickness), Tb.sp (trabecular separation), Tb.N (trabecular number). The analysis area containing the fixation nails was analyzed using a 10x microscope. Field of view splicing analysis was performed, and the corresponding relevant parameter values were exported from the bone tissue morphology analysis and measurement system.

Statistical analysis

The experimental data were analyzed using statistical software (SPSS 27.0, USA). Levene's test was used to assess the normal distribution and homogeneity of variance of the measurement data of the un-MAO surface treatment group (Group A) and the MAO surface treatment group (Group B) at 4 w, 8 w, and 12 weeks. All

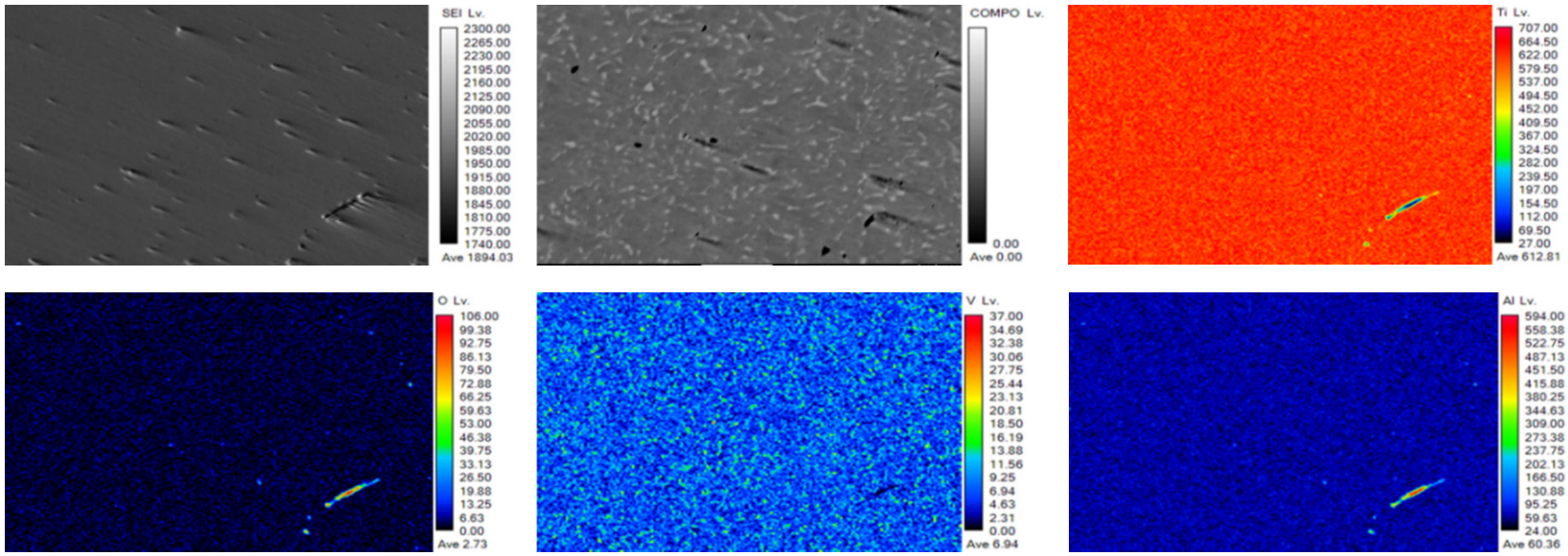

Figure 2. Surface element content of the threaded part of group A microscrews. Surface element content map.

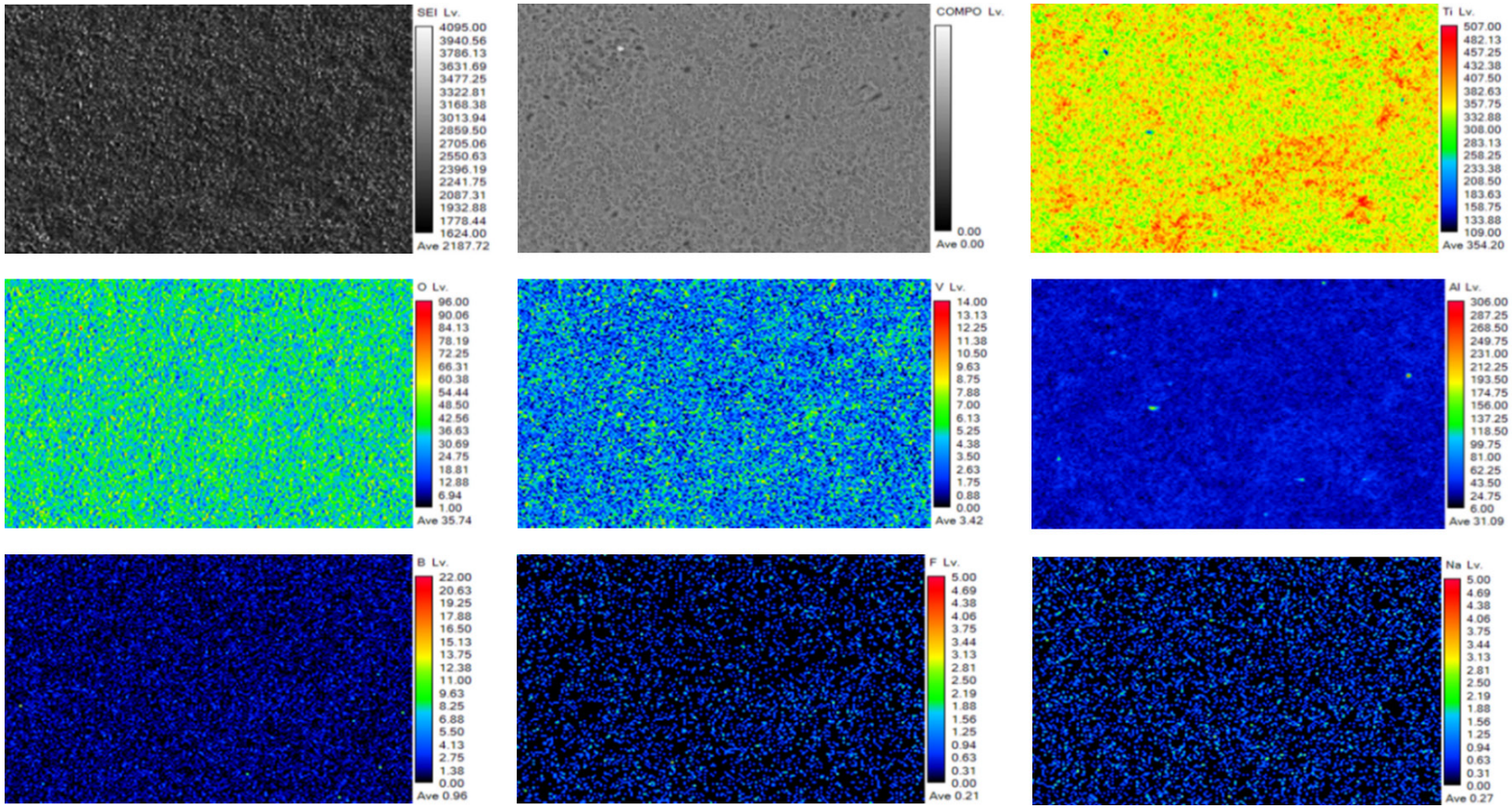

Figure 3. Surface element content of the threaded part of group B microscrews. Surface element content map.

Table 1. Surface element content of Group B microscrews

Element	Al	Na	Ti	F	V	O	B	Total
Mass (%)	3.262	0.030	46.288	0.747	2.077	49.070	1.117	102.591
Atom (%)	2.7864	0.0305	22.2721	0.9065	0.9365	70.6836	2.3814	100.0000

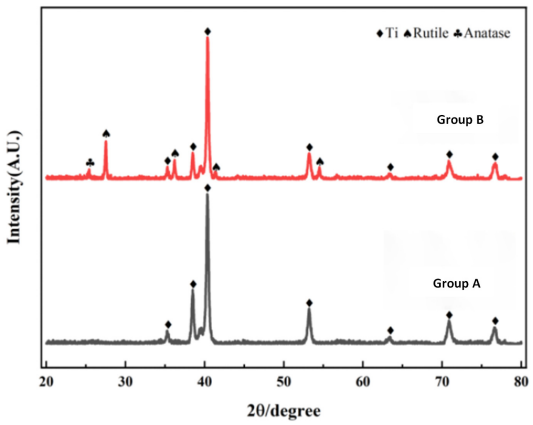

Figure 4. Comparison of the surface crystals of group A and B microscrews.

data conformed to a normal distribution and homogeneity of variance. Comparisons between Group A and Group B were performed using an independent sample t-test, while a one-way ANOVA was used to evaluate the differences among the 4-week, 8-week, and 12-week groups. A P value < 0.05 was considered significant.

Results

SEM (Scanning Electron Microscope) characterization of the threaded part of the micro-implant microscrews in Group A and Group B

The surface of the threaded part of the Group B microscrews appeared uneven, displaying pores with relatively uniform diameters, resembling a "crater" like morphology (**Figure 1A-C**).

Electron microprobe elemental analysis of the threaded parts of the micro-implant microscrews in Groups A and B

The results of electron microprobe probing revealed that Ti, Al, V, and O were present on the surface of the Group A microscrews (**Figure 2**). In contrast the surface of Group B screws contained Na, F, and B elements from the electrolyte, in addition to the elements detected in Group A (**Figure 3**). Notably the O content in Group B was significantly higher due to the oxidized layer generated by MAO treatment (**Table 1**).

Comparison of the surface crystal phases of the threaded part of the micro-implant microscrews in Groups A and B

The surface crystalline phase of Group A microscrews consisted primarily of Ti, whereas Group B exhibited a rutile phase along with a small amount of anatase phase in addition to Ti (**Figure 4**).

Comparison of the wettability of the threaded part of the micro-implant microscrews in Groups A and B

As shown in **Figure 5**, the hydrophilic contact angle of the threaded part of Group A microscrews was greater than that of Group B microscrews, indicating superior hydrophilicity in Group B.

Comparison of the roughness (Ra value) of the threaded part of the micro-implant microscrews in Groups A and B

Roughness measurements revealed an Ra value of 0.047 μm for the surface of the threaded part in Group A microscrews, compared with a Ra value of 0.312 μm for the coated surface of the Group B microscrews, thereby indicating that the threaded portion of Group B screws had greater roughness than that of Group A (**Figure 6**).

Coating bond strength of the threaded part of Group B microscrews

SEM images revealed no obvious surface detachment on the threaded portion of Group B microscrews, and the cuts appeared relatively flush (**Figure 7**). According to the American Society for Testing and Materials (ASTM) method rating criteria [15], the scribed edges were smooth, with no coating shedding at the intersections, resulting in the highest grade of 5 B.

The volume ratio, trabecular bone thickness value, and trabecular bone value of the fixation

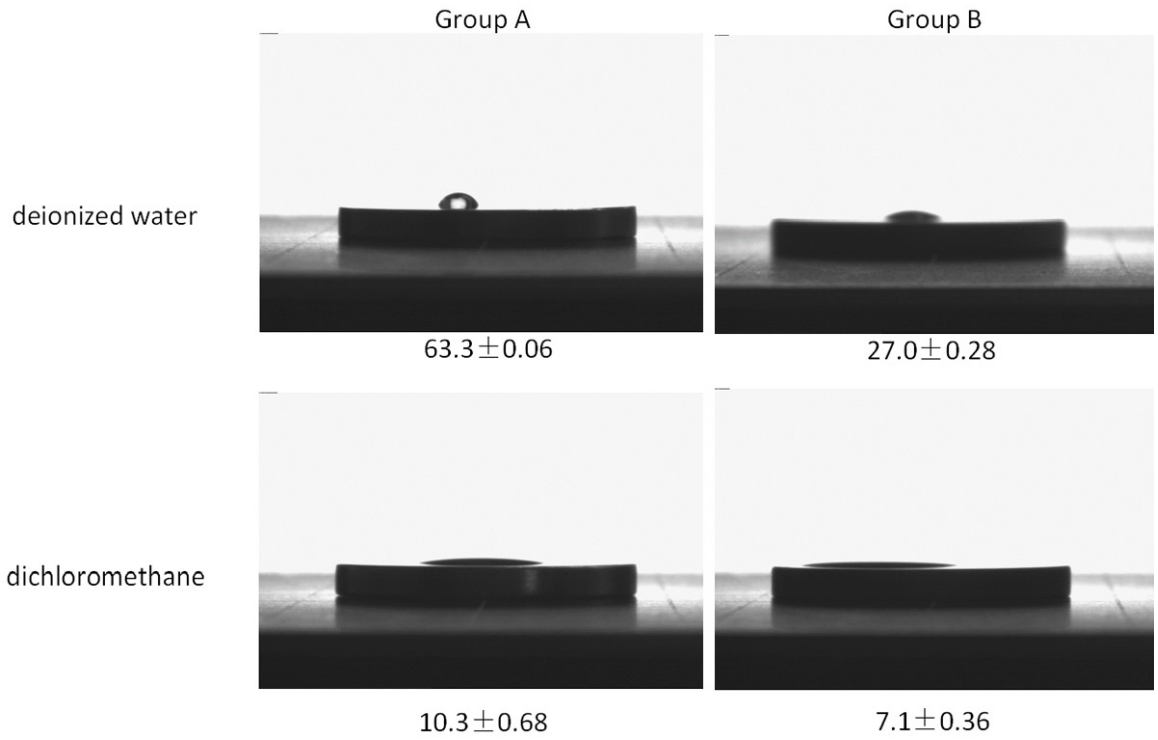

Figure 5. Comparison of contact angle of group A and B microscrews.

screws in Groups A and B at 4, 8, and 12 weeks were all significant ($P < 0.05$). However, comparison of retention screws between Groups A and B at the same time points revealed that only the volume ratio at 8 weeks was significant ($P < 0.05$), with no significance at 4 weeks or 12 weeks ($P > 0.05$) (**Tables 2** and **3**).

The bone combination rates of the retention screws were as follows: at 4 weeks, 0.32±0.08 in group A and 0.33±0.03 in group B; at 8 weeks, 0.34±0.08 in Group A and 0.36±0.00 in Group B; and at 12 weeks, 0.36±0.11 in Group A and 0.39±0.05 in Group B. Notably, there was no significant difference between Groups A and B at 4, 8, or 12 weeks ($P = 0.284$, 0.628, and 0.589 respectively). Similarly, there was also no significant difference in the bone combination rate across the three time points ($P = 0.085$).

Discussion

Implants with MAO coating exhibit a greater bone-implant contact area and increased new bone attachment. Over time, the immature new bone matures into a lamellar dense bone and irregular dense bone, eventually penetrating the porous structure of the MAO coating and becoming firmly anchored within its porous cavity [16]. The interconnected micropores on the MAO coating are equivalent to a three-dimensional scaffolding structure that increases the attachment area for tissue cells, which facilitates bone tissue growth into the pores, promotes cell adhesion and extension, and provides an optimal material environment for cell binding and survival [17]. The newly formed symbiotic bone tissue is denser and capable of withstanding greater shear force [18]. The results of this study revealed that the micro-implant pegs with MAO coating exhibited a significant increase in the amount of new bone compared to the control group at 4, 8, and 12 weeks in the animal model. However, the difference was not statistically significant except for BV/TV at 8 weeks.

The state of osseointegration is critical for the stability of the micro-screws. Good osseointegration establishes a direct connection between the bone tissue and micro-screw, enabling it to bear substantial loads without the risk of dislodgement [19]. Additionally, enhancing the mechanical locking force between the micro-screws and the bone, along with the osteoblast

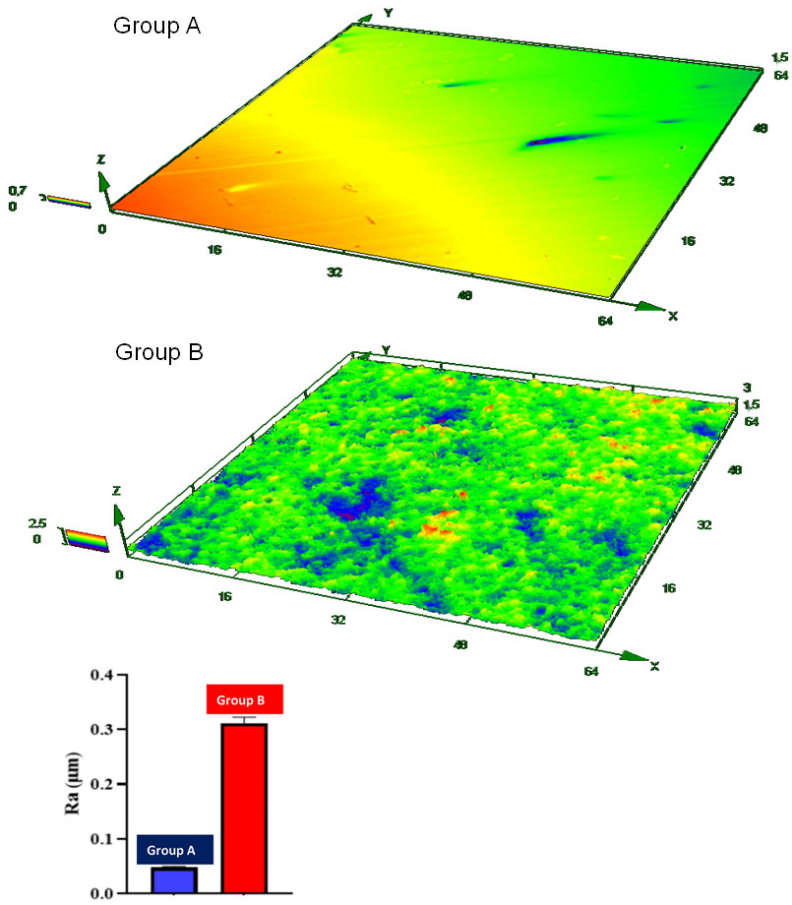

Figure 6. Comparison of 3D topography maps and roughness (Ra) values.

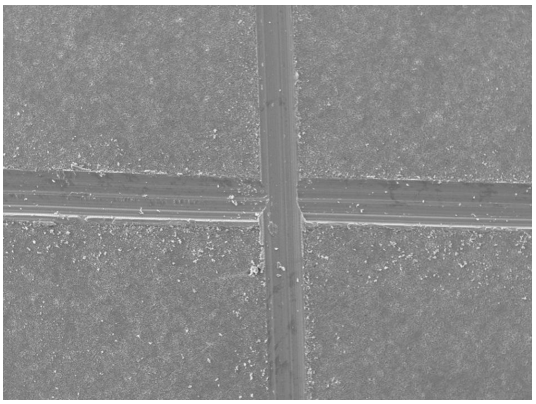

Figure 7. SEM image of Group B peg cross-hatched grid.

activity and osteogenic differentiation ability, is extremely essential for the osseointegration of the micro-implant microscrews. The morphology of the surface of the MAO surface-treated micro-implant microscrews affects the osteoblast response, enhancing the adhesion and proliferation of preosteoblasts, and increasing the hydrophilicity of the microscrews' surface. This increase in hydrophilicity enhances the protein adsorption capacity and promotes osteoblast growth and differentiation [20]. Animal experiments revealed that the implantation of MAO surface-treated Ti-alloy into the bones of healthy adult male New Zealand rabbits led to prominent new bone formation around the microscrews, thereby demonstrating the effectiveness of the MAO coating in promoting osseointegration and consistent with the findings of previous studies [21, 22].

In orthodontic treatment, the initial stability of the micro-screws immediately after their implantation is entirely dependent on the mechanical locking connection between the screw and the bone, referred to as the initial stability of the micro-implants [23]. This initial stability relies primarily on the contact area between the bone tissue and the micro-screw, guaranteeing stability during the first weeks after implantation. However, traditional smooth-surfaced micro-screws are often unstable at first, while this initial stability can be increased by enhancing the roughness of the surface. The formation of new bone around the micro-implant, together with osseointegration, further increases the stability, a phenomenon termed "secondary stability" [24]. The successful implantation of microscrews in the clinic relies on a combination of primary and secondary stability [25]. New bone forms and remodels around the microscrews, resulting in a significantly higher bone-implant contact value (BIC value) compared to micro-implant microscrews with smooth surfaces [26]. The BIC is an essential indicator of primary stability, which provides fixation strength, and secondary stability, which supports osseointegration. Optimal micro-implant osseointegration ensu-

Table 2. Comparison of the amount of new bone around the microscrews within the 4 w, 8 w, and 12 w groups

Parameter	4 w		T-value	*P*-value	8 w		T-value	*P*-value	12 w		T-value	*P*-value
	Group A	Group B			Group A	Group B			Group A	Group B		
BV/TV	8.57±2.47	9.88±2.03	-0.823	0.443	10.17±0.72	12.32±1.00	-3.497	0.015	13.71±1.67	15.1±1.99	-0.232	0.327
Tb.Th (um)	29.1±3.62	36.5±7.99	-1.687	0.163	34.84±3.09	38.89±5.31	-1.137	0.247	63.24±4.76	70.52±9.30	1.787	0.229
Tb.Sp (um)	324.55±78.01	332.65±30.63	-0.193	0.865	307.55±15.15	276.98±33.39	1.667	0.168	470.53±79.39	422.71±121.40	0.659	0.538
Tb.N (mm)	2.93±0.64	2.73±0.24	0.605	0.579	2.93±0.14	3.2±0.43	-1.239	0.289	1.8±0.29	2.15±0.60	-1.029	0.358

Table 3. Comparison of new bone volume of microscrews between 4 w, 8 w, and 12 w groups

Parameter	Group A			*F-value*	*P-value*	Group B			*F-value*	*P-value*
	4 w	8 w	12 w			4 w	8 w	12 w		
BV/TV	8.57±2.47	10.17±0.72	13.71±1.67	8.476	0.034	9.88±2.03	12.32±1.00	15.1±1.99	9.044	0.009
Tb.Th (um)	29.1±3.62	34.84±3.09	63.24±4.76	11.327	0.005	36.5±7.99	38.89±5.31	70.52±9.30	12.215	0.001
Tb.Sp (um)	324.55±78.01	307.55±15.15	470.53±79.39	7.633	0.088	332.65±30.63	276.98±33.39	422.71±121.40	3.864	0.061
Tb.N (mm)	2.93±0.64	2.93±0.14	1.8±0.29	9.957	0.008	2.73±0.24	3.2±0.43	2.15±0.60	5.552	0.027

res clinically stable support while allowing for easy removal [27]. After MAO surface treatment, the surface of micro-implant microscrews exhibited a porous coating with a 'volcanic crater' like morphology, good wettability, and increased roughness. These features promoted the stabilization of the micro-implant microscrews, without a significant difference in the osseointegration rate. Partial osseointegration also facilitated the removal of the micro-implant microscrews.

It is noteworthy that the volume of new bone surrounding the micro-screws was significantly increased at 4, 8, and 12 weeks, indicating that the micro-arc oxidation surface treatment can enhance the stability of micro-implants in terms of their micro-screws.

There were several limitations to this study. First, the sample size was relatively small, potentially leading to errors in the experimental data. Second, in the experiment, CT scans were not conducted to assess the structure of the bone tissue, and data on bone density measurement were not collected. Further investigation is needed to address these issues to verify the current conclusions.

Acknowledgements

This work was supported by Dalian Science and Technology Innovation Fund (2022JJ13SN069).

Written informed consent was obtained from the patient for publication of this case report and any accompanying images.

Disclosure of conflict of interest

None.

Address correspondence to: Wantian Xu, Nanjing Stomatological Hospital, Affiliated Hospital of Medical School, Research Institute of Stomatology, Nanjing University, Nanjing, Jiangsu, China. Tel: +86-25-86220179; E-mail: chinaxuwantian@163.com; Lin Liu, Department of Orthodontics, Dalian Stomatological Hospital, Graduate School of Dalian Medical University, Dalian, Liaoning, China. Tel: +86-411-84651356; E-mail: llin3333@163.com

References

[1] Chen YJ, Chang HH, Lin HY, Lai EH, Hung HC and Yao CC. Stability of miniplates and miniscrews used for orthodontic anchorage: experience with 492 temporary anchorage devices. Clin Oral Implants Res 2008; 19: 1188-1196.

[2] Melo AC, Andrighetto AR, Hirt SD, Bongiolo AL, Silva SU and Silva MA. Risk factors associated with the failure of miniscrews - A ten-year cross sectional study. Braz Oral Res 2016; 30: e124.

[3] Gurdan Z and Szalma J. Evaluation of the success and complication rates of self-drilling orthodontic mini-implants. Niger J Clin Pract 2018; 21: 546-552.

[4] Popova NV, Arsenina OI, Lebedenko IY, Rusanov FS, Khvorostenko EA and Glukhova NV. The experimental study of a Russian orthodontic mini-screw. Stomatologiia (Mosk) 2021; 100: 7-12.

[5] Ichinohe M, Motoyoshi M, Inaba M, Uchida Y, Kaneko M, Matsuike R and Shimizu N. Risk factors for failure of orthodontic mini-screws placed in the median palate. J Oral Sci 2019; 61: 13-18.

[6] Xu N, Fu J, Zhao L, Chu PK and Huo K. Biofunctional elements incorporated nano/microstructured coatings on titanium implants with enhanced osteogenic and antibacterial performance. Adv Healthc Mater 2020; 9: e2000681.

[7] Sanchez-Perez A, Cachazo-Jiménez C, Sánchez-Matás C, Martín-de-Llano JJ, Davis S and Carda-Batalla C. Effects of ultraviolet photoactivation on osseointegration of commercial pure titanium dental implant after 8 weeks in a rabbit model. J Oral Implantol 2020; 46: 101-107.

[8] Nyan M, Hao J, Miyahara T, Noritake K, Rodriguez R and Kasugai S. Accelerated and enhanced bone formation on novel simvastatin-loaded porous titanium oxide surfaces. Clin Implant Dent Relat Res 2014; 16: 675-683.

[9] Li G, Cao H, Zhang W, Ding X, Yang G, Qiao Y, Liu X and Jiang X. Enhanced osseointegration of hierarchical micro/nanotopographic titanium fabricated by microarc oxidation and electrochemical treatment. ACS Appl Mater Interfaces 2016; 8: 3840-3852.

[10] Nyan M, Hao J, Miyahara T, Noritake K, Rodriguez R and Kasugai S. Accelerated and enhanced bone formation on novel simvastatin-loaded porous titanium oxide surfaces. Clin Implant Dent Relat Res 2014; 16: 675-683.

[11] Zhang B, Li J, He L, Huang H and Weng J. Biosurface coated titanium scaffolds with cancellous bone-like biomimetic structure for enhanced bone tissue regeneration. Acta Biomater 2020; 114: 431-448.

[12] Pesode P and Barve S. Surface modification of titanium and titanium alloy by plasma electrolytic oxidation process for biomedical applications: a review. Materials Today: Proceedings 2021; 46: 594-602.

[13] Li G, Ma F, Liu P, Qi S, Li W, Zhang K and Chen X. Review of micro-arc oxidation of titanium alloys: mechanism, properties and applications. J Alloys Compd 2023; 948: 169773.
[14] Hotchkiss KM, Reddy GB, Hyzy SL, Schwartz Z, Boyan BD and Olivares-Navarrete R. Titanium surface characteristics, including topography and wettability, alter macrophage activation. Acta Biomater 2016; 31: 425-434.
[15] Shi L, Ning W and Luo L. Comparison among different standards for adhesion test of coating. Shanghai Coatings 2017.
[16] Ni R, Jing Z, Xiong C, Meng D, Wei C and Cai H. Effect of micro-arc oxidation surface modification of 3D-printed porous titanium alloys on biological properties. Ann Transl Med 2022; 10: 710.
[17] Wang LJ, Ni XH, Zhang F, Peng Z, Yu FX, Zhang LB, Li B, Jiao Y, Li YK, Yang B, Zhu XY and Zhao QM. Osteoblast response to copper-doped microporous coatings on titanium for improved bone integration. Nanoscale Res Lett 2021; 16: 146.
[18] Chen HT, Lin HI, Chung CJ, Tang CH and He JL. Osseointegrating and phase-oriented micro-arc-oxidized titanium dioxide bone implants. J Appl Biomater Funct Mater 2021; 19: 22808000211006878.
[19] Huang L, Cai B, Huang Y, Wang J, Zhu C, Shi K, Song Y, Feng G, Liu L and Zhang L. Comparative study on 3D printed Ti6Al4V scaffolds with surface modifications using hydrothermal treatment and microarc oxidation to enhance osteogenic activity. ACS Omega 2021; 6: 1465-1476.
[20] Tang J, Wu Z, Yao X, Zhou Y, Xiong Y, Li Y, Xu J, Dargusch MS and Yan M. From bio-inertness to osseointegration and antibacterial activity: a one-step micro-arc oxidation approach for multifunctional Ti implants fabricated by additive manufacturing. Materials & Design 2022; 221: 110962.
[21] Xiu P, Jia Z, Lv J, Yin C, Cheng Y, Zhang K, Song C, Leng H, Zheng Y, Cai H and Liu Z. Tailored surface treatment of 3D printed porous Ti6Al4V by microarc oxidation for enhanced osseointegration via optimized bone in-growth patterns and interlocked bone/implant interface. ACS Appl Mater Interfaces 2016; 8: 17964-17975.
[22] Zhao QM, Li XK, Guo S, Wang N, Liu WW, Shi L and Guo Z. Osteogenic activity of a titanium surface modified with silicon-doped titanium dioxide. Mater Sci Eng C Mater Biol Appl 2020; 110: 110682.
[23] Jain S, Ponnada S and Chandrasekhar G. Comparison of biomechanical properties of surface-treated and untreated machined orthodontic mini-implants: an in vitro study. J Indian Orthod Soc 2023; 57: 17-22.
[24] Al-Thomali Y, Basha S and Mohamed RN. Effect of surface treatment on the mechanical stability of orthodontic miniscrews. Angle Orthod 2022; 92: 127-136.
[25] Byeon SM, Jeon J, Jang YS, Jeon WY, Lee MH, Jeon YM, Kim JG and Bae TS. Evaluation of osseointegration of Ti-6Al-4V alloy orthodontic mini-screws with ibandronate-loaded TiO2 nanotube layer. Dent Mater J 2023; 42: 610-616.
[26] Maino BG, Di Blasio A, Spadoni D, Ravanetti F, Galli C, Cacchioli A, Katsaros C and Gandolfini M. The integration of orthodontic miniscrews under mechanical loading: a pre-clinical study in rabbit. Eur J Orthod 2017; 39: 519-527.
[27] Gracco A, Cirignaco A, Cozzani M, Boccaccio A, Pappalettere C and Vitale G. Numerical/experimental analysis of the stress field around miniscrews for orthodontic anchorage. Eur J Orthod 2009; 31: 12-20.